

Search for Lepton-Flavor Violation in the Decay $\tau^- \rightarrow \ell^- \ell^+ \ell^-$

B. Aubert,¹ R. Barate,¹ D. Boutigny,¹ F. Couderc,¹ J.-M. Gaillard,¹ A. Hicheur,¹ Y. Karyotakis,¹ J. P. Lees,¹ V. Tisserand,¹ A. Zghiche,¹ A. Palano,² A. Pompili,² J. C. Chen,³ N. D. Qi,³ G. Rong,³ P. Wang,³ Y. S. Zhu,³ G. Eigen,⁴ I. Ofte,⁴ B. Stugu,⁴ G. S. Abrams,⁵ A. W. Borgland,⁵ A. B. Breon,⁵ D. N. Brown,⁵ J. Button-Shafer,⁵ R. N. Cahn,⁵ E. Charles,⁵ C. T. Day,⁵ M. S. Gill,⁵ A. V. Gritsan,⁵ Y. Groysman,⁵ R. G. Jacobsen,⁵ R. W. Kadel,⁵ J. Kadyk,⁵ L. T. Kerth,⁵ Yu. G. Kolomensky,⁵ G. Kukartsev,⁵ C. LeClerc,⁵ M. E. Levi,⁵ G. Lynch,⁵ L. M. Mir,⁵ P. J. Oddone,⁵ T. J. Orimoto,⁵ M. Pripstein,⁵ N. A. Roe,⁵ M. T. Ronan,⁵ V. G. Shelkov,⁵ A. V. Telnov,⁵ W. A. Wenzel,⁵ K. Ford,⁶ T. J. Harrison,⁶ C. M. Hawkes,⁶ S. E. Morgan,⁶ A. T. Watson,⁶ N. K. Watson,⁶ M. Fritsch,⁷ K. Goetzen,⁷ T. Held,⁷ H. Koch,⁷ B. Lewandowski,⁷ M. Pelizaeus,⁷ M. Steinke,⁷ J. T. Boyd,⁸ N. Chevalier,⁸ W. N. Cottingham,⁸ M. P. Kelly,⁸ T. E. Latham,⁸ F. F. Wilson,⁸ K. Abe,⁹ T. Cuhadar-Donszelmann,⁹ C. Hearty,⁹ T. S. Mattison,⁹ J. A. McKenna,⁹ D. Thiessen,⁹ P. Kyberd,¹⁰ L. Teodorescu,¹⁰ V. E. Blinov,¹¹ A. D. Bukin,¹¹ V. P. Druzhinin,¹¹ V. B. Golubev,¹¹ V. N. Ivanchenko,¹¹ E. A. Kravchenko,¹¹ A. P. Onuchin,¹¹ S. I. Serednyakov,¹¹ Yu. I. Skovpen,¹¹ E. P. Solodov,¹¹ A. N. Yushkov,¹¹ D. Best,¹² M. Bruinsma,¹² M. Chao,¹² I. Eschrich,¹² D. Kirkby,¹² A. J. Lankford,¹² M. Mandelkern,¹² R. K. Mommsen,¹² W. Roethel,¹² D. P. Stoker,¹² C. Buchanan,¹³ B. L. Hartfiel,¹³ J. W. Gary,¹⁴ B. C. Shen,¹⁴ K. Wang,¹⁴ D. del Re,¹⁵ H. K. Hadavand,¹⁵ E. J. Hill,¹⁵ D. B. MacFarlane,¹⁵ H. P. Paar,¹⁵ Sh. Rahatlou,¹⁵ V. Sharma,¹⁵ J. W. Berryhill,¹⁶ C. Campagnari,¹⁶ B. Dahmes,¹⁶ S. L. Levy,¹⁶ O. Long,¹⁶ A. Lu,¹⁶ M. A. Mazur,¹⁶ J. D. Richman,¹⁶ W. Verkerke,¹⁶ T. W. Beck,¹⁷ A. M. Eisner,¹⁷ C. A. Heusch,¹⁷ W. S. Lockman,¹⁷ T. Schalk,¹⁷ R. E. Schmitz,¹⁷ B. A. Schumm,¹⁷ A. Seiden,¹⁷ P. Spradlin,¹⁷ D. C. Williams,¹⁷ M. G. Wilson,¹⁷ J. Albert,¹⁸ E. Chen,¹⁸ G. P. Dubois-Felsmann,¹⁸ A. Dvoretzskii,¹⁸ D. G. Hitlin,¹⁸ I. Narsky,¹⁸ T. Piatenko,¹⁸ F. C. Porter,¹⁸ A. Ryd,¹⁸ A. Samuel,¹⁸ S. Yang,¹⁸ S. Jayatilake,¹⁹ G. Mancinelli,¹⁹ B. T. Meadows,¹⁹ M. D. Sokoloff,¹⁹ T. Abe,²⁰ F. Blanc,²⁰ P. Bloom,²⁰ S. Chen,²⁰ P. J. Clark,²⁰ W. T. Ford,²⁰ U. Nauenberg,²⁰ A. Olivas,²⁰ P. Rankin,²⁰ J. G. Smith,²⁰ W. C. van Hoek,²⁰ L. Zhang,²⁰ J. L. Harton,²¹ T. Hu,²¹ A. Soffer,²¹ W. H. Toki,²¹ R. J. Wilson,²¹ D. Altenburg,²² T. Brandt,²² J. Brose,²² T. Colberg,²² M. Dickopp,²² E. Feltresi,²² A. Hauke,²² H. M. Lacker,²² E. Maly,²² R. Müller-Pfefferkorn,²² R. Nogowski,²² S. Otto,²² J. Schubert,²² K. R. Schubert,²² R. Schwierz,²² B. Spaan,²² D. Bernard,²³ G. R. Bonneaud,²³ F. Brochard,²³ P. Grenier,²³ Ch. Thiebaut,²³ G. Vasileiadis,²³ M. Verderi,²³ D. J. Bard,²⁴ A. Khan,²⁴ D. Lavin,²⁴ F. Muheim,²⁴ S. Playfer,²⁴ M. Andreotti,²⁵ V. Azzolini,²⁵ D. Bettoni,²⁵ C. Bozzi,²⁵ R. Calabrese,²⁵ G. Cibinetto,²⁵ E. Luppi,²⁵ M. Negrini,²⁵ A. Sarti,²⁵ E. Treadwell,²⁶ R. Baldini-Ferrolì,²⁷ A. Calcaterra,²⁷ R. de Sangro,²⁷ G. Finocchiaro,²⁷ P. Patteri,²⁷ M. Piccolo,²⁷ A. Zallo,²⁷ A. Buzzo,²⁸ R. Capra,²⁸ R. Contri,²⁸ G. Crosetti,²⁸ M. Lo Vetere,²⁸ M. Macri,²⁸ M. R. Monge,²⁸ S. Passaggio,²⁸ C. Patrignani,²⁸ E. Robutti,²⁸ A. Santroni,²⁸ S. Tosi,²⁸ S. Bailey,²⁹ G. Brandenburg,²⁹ M. Morii,²⁹ E. Won,²⁹ R. S. Dubitzky,³⁰ U. Langenegger,³⁰ W. Bhimji,³¹ D. A. Bowerman,³¹ P. D. Dauncey,³¹ U. Egede,³¹ J. R. Gaillard,³¹ G. W. Morton,³¹ J. A. Nash,³¹ G. P. Taylor,³¹ G. J. Grenier,³² S.-J. Lee,³² U. Mallik,³² J. Cochran,³³ H. B. Crawley,³³ J. Lamsa,³³ W. T. Meyer,³³ S. Prell,³³ E. I. Rosenberg,³³ J. Yi,³³ M. Davier,³⁴ G. Grosdidier,³⁴ A. Höcker,³⁴ S. Laplace,³⁴ F. Le Diberder,³⁴ V. Lepeltier,³⁴ A. M. Lutz,³⁴ T. C. Petersen,³⁴ S. Plaszczynski,³⁴ M. H. Schune,³⁴ L. Tantot,³⁴ G. Wormser,³⁴ C. H. Cheng,³⁵ D. J. Lange,³⁵ M. C. Simani,³⁵ D. M. Wright,³⁵ A. J. Bevan,³⁶ J. P. Coleman,³⁶ J. R. Fry,³⁶ E. Gabathuler,³⁶ R. Gamet,³⁶ M. Kay,³⁶ R. J. Parry,³⁶ D. J. Payne,³⁶ R. J. Sloane,³⁶ C. Touramanis,³⁶ J. J. Back,³⁷ P. F. Harrison,³⁷ G. B. Mohanty,³⁷ C. L. Brown,³⁸ G. Cowan,³⁸ R. L. Flack,³⁸ H. U. Flaecher,³⁸ S. George,³⁸ M. G. Green,³⁸ A. Kurup,³⁸ C. E. Marker,³⁸ T. R. McMahon,³⁸ S. Ricciardi,³⁸ F. Salvatore,³⁸ G. Vaitas,³⁸ M. A. Winter,³⁸ D. Brown,³⁹ C. L. Davis,³⁹ J. Allison,⁴⁰ N. R. Barlow,⁴⁰ R. J. Barlow,⁴⁰ P. A. Hart,⁴⁰ M. C. Hodgkinson,⁴⁰ G. D. Lafferty,⁴⁰ A. J. Lyon,⁴⁰ J. C. Williams,⁴⁰ A. Farbin,⁴¹ W. D. Hulsbergen,⁴¹ A. Jawahery,⁴¹ D. Kovalskyi,⁴¹ C. K. Lae,⁴¹ V. Lillard,⁴¹ D. A. Roberts,⁴¹ G. Blaylock,⁴² C. Dallapiccola,⁴² K. T. Flood,⁴² S. S. Hertzbach,⁴² R. Kofler,⁴² V. B. Koptchev,⁴² T. B. Moore,⁴² S. Saremi,⁴² H. Staengle,⁴² S. Willocq,⁴² R. Cowan,⁴³ G. Sciolla,⁴³ F. Taylor,⁴³ R. K. Yamamoto,⁴³ D. J. J. Mangeol,⁴⁴ P. M. Patel,⁴⁴ S. H. Robertson,⁴⁴ A. Lazzaro,⁴⁵ F. Palombo,⁴⁵ J. M. Bauer,⁴⁶ L. Cremaldi,⁴⁶ V. Eschenburg,⁴⁶ R. Godang,⁴⁶ R. Kroeger,⁴⁶ J. Reidy,⁴⁶ D. A. Sanders,⁴⁶ D. J. Summers,⁴⁶ H. W. Zhao,⁴⁶ S. Brunet,⁴⁷ D. Côté,⁴⁷ P. Taras,⁴⁷ H. Nicholson,⁴⁸ C. Cartaro,⁴⁹ N. Cavallo,⁴⁹ F. Fabozzi,^{49,*} C. Gatto,⁴⁹ L. Lista,⁴⁹ D. Monorchio,⁴⁹ P. Paolucci,⁴⁹ D. Piccolo,⁴⁹ C. Sciacca,⁴⁹ M. Baak,⁵⁰ G. Raven,⁵⁰ L. Wilden,⁵⁰ C. P. Jessop,⁵¹ J. M. LoSecco,⁵¹ T. A. Gabriel,⁵² T. Allmendinger,⁵³ B. Brau,⁵³ K. K. Gan,⁵³ K. Honscheid,⁵³ D. Hufnagel,⁵³ H. Kagan,⁵³ R. Kass,⁵³ T. Pulliam,⁵³ R. Ter-Antonyan,⁵³ Q. K. Wong,⁵³ J. Brau,⁵⁴ R. Frey,⁵⁴ O. Igonkina,⁵⁴ C. T. Potter,⁵⁴ N. B. Sinev,⁵⁴ D. Strom,⁵⁴ E. Torrence,⁵⁴ F. Colecchia,⁵⁵ A. Dorigo,⁵⁵ F. Galeazzi,⁵⁵ M. Margoni,⁵⁵ M. Morandin,⁵⁵ M. Posocco,⁵⁵ M. Rotondo,⁵⁵

F. Simonetto,⁵⁵ R. Stroili,⁵⁵ G. Tiozzo,⁵⁵ C. Voci,⁵⁵ M. Benayoun,⁵⁶ H. Briand,⁵⁶ J. Chauveau,⁵⁶ P. David,⁵⁶ Ch. de la Vaissière,⁵⁶ L. Del Buono,⁵⁶ O. Hamon,⁵⁶ M. J. J. John,⁵⁶ Ph. Leruste,⁵⁶ J. Ocariz,⁵⁶ M. Pivk,⁵⁶ L. Roos,⁵⁶ S. T'Jampens,⁵⁶ G. Therin,⁵⁶ P. F. Manfredi,⁵⁷ V. Re,⁵⁷ P. K. Behera,⁵⁸ L. Gladney,⁵⁸ Q. H. Guo,⁵⁸ J. Panetta,⁵⁸ F. Anulli,^{27,59} M. Biasini,⁵⁹ I. M. Peruzzi,^{27,59} M. Pioppi,⁵⁹ C. Angelini,⁶⁰ G. Batignani,⁶⁰ S. Bettarini,⁶⁰ M. Bondioli,⁶⁰ F. Bucci,⁶⁰ G. Calderini,⁶⁰ M. Carpinelli,⁶⁰ V. Del Gamba,⁶⁰ F. Forti,⁶⁰ M. A. Giorgi,⁶⁰ A. Lusiani,⁶⁰ G. Marchiori,⁶⁰ F. Martinez-Vidal,^{60,†} M. Morganti,⁶⁰ N. Neri,⁶⁰ E. Paoloni,⁶⁰ M. Rama,⁶⁰ G. Rizzo,⁶⁰ F. Sandrelli,⁶⁰ J. Walsh,⁶⁰ M. Haire,⁶¹ D. Judd,⁶¹ K. Paick,⁶¹ D. E. Wagoner,⁶¹ N. Danielson,⁶² P. Elmer,⁶² C. Lu,⁶² V. Miftakov,⁶² J. Olsen,⁶² A. J. S. Smith,⁶² E. W. Varnes,⁶² F. Bellini,⁶³ G. Cavoto,^{62,63} R. Faccini,⁶³ F. Ferrarotto,⁶³ F. Ferroni,⁶³ M. Gaspero,⁶³ L. Li Gioi,⁶³ M. A. Mazzoni,⁶³ S. Morganti,⁶³ M. Pierini,⁶³ G. Piredda,⁶³ F. Safai Tehrani,⁶³ C. Voena,⁶³ S. Christ,⁶⁴ G. Wagner,⁶⁴ R. Waldi,⁶⁴ T. Adye,⁶⁵ N. De Groot,⁶⁵ B. Franek,⁶⁵ N. I. Geddes,⁶⁵ G. P. Gopal,⁶⁵ E. O. Olaiya,⁶⁵ S. M. Xella,⁶⁵ R. Aleksan,⁶⁶ S. Emery,⁶⁶ A. Gaidot,⁶⁶ S. F. Ganzhur,⁶⁶ P.-F. Giraud,⁶⁶ G. Hamel de Monchenault,⁶⁶ W. Kozanecki,⁶⁶ M. Langer,⁶⁶ M. Legendre,⁶⁶ G. W. London,⁶⁶ B. Mayer,⁶⁶ G. Schott,⁶⁶ G. Vasseur,⁶⁶ Ch. Yèche,⁶⁶ M. Zito,⁶⁶ M. V. Purohit,⁶⁷ A. W. Weidemann,⁶⁷ F. X. Yumiceva,⁶⁷ D. Aston,⁶⁸ R. Bartoldus,⁶⁸ N. Berger,⁶⁸ A. M. Boyarski,⁶⁸ O. L. Buchmueller,⁶⁸ M. R. Convery,⁶⁸ M. Cristinziani,⁶⁸ G. De Nardo,⁶⁸ D. Dong,⁶⁸ J. Dorfan,⁶⁸ D. Dujmic,⁶⁸ W. Dunwoodie,⁶⁸ E. E. Elsen,⁶⁸ R. C. Field,⁶⁸ T. Glanzman,⁶⁸ S. J. Gowdy,⁶⁸ T. Hadig,⁶⁸ V. Halyo,⁶⁸ T. Hryn'ova,⁶⁸ W. R. Innes,⁶⁸ M. H. Kelsey,⁶⁸ P. Kim,⁶⁸ M. L. Kocian,⁶⁸ D. W. G. S. Leith,⁶⁸ J. Libby,⁶⁸ S. Luitz,⁶⁸ V. Luth,⁶⁸ H. L. Lynch,⁶⁸ H. Marsiske,⁶⁸ R. Messner,⁶⁸ D. R. Muller,⁶⁸ C. P. O'Grady,⁶⁸ V. E. Ozcan,⁶⁸ A. Perazzo,⁶⁸ M. Perl,⁶⁸ S. Petrak,⁶⁸ B. N. Ratcliff,⁶⁸ A. Roodman,⁶⁸ A. A. Salnikov,⁶⁸ R. H. Schindler,⁶⁸ J. Schwiening,⁶⁸ G. Simi,⁶⁸ A. Snyder,⁶⁸ A. Soha,⁶⁸ J. Stelzer,⁶⁸ D. Su,⁶⁸ M. K. Sullivan,⁶⁸ J. Va'vra,⁶⁸ S. R. Wagner,⁶⁸ M. Weaver,⁶⁸ A. J. R. Weinstein,⁶⁸ W. J. Wisniewski,⁶⁸ M. Wittgen,⁶⁸ D. H. Wright,⁶⁸ C. C. Young,⁶⁸ P. R. Burchat,⁶⁹ A. J. Edwards,⁶⁹ T. I. Meyer,⁶⁹ B. A. Petersen,⁶⁹ C. Roat,⁶⁹ S. Ahmed,⁷⁰ M. S. Alam,⁷⁰ J. A. Ernst,⁷⁰ M. A. Saeed,⁷⁰ M. Saleem,⁷⁰ F. R. Wappler,⁷⁰ W. Bugg,⁷¹ M. Krishnamurthy,⁷¹ S. M. Spanier,⁷¹ R. Eckmann,⁷² H. Kim,⁷² J. L. Ritchie,⁷² A. Satpathy,⁷² R. F. Schwitters,⁷² J. M. Izen,⁷³ I. Kitayama,⁷³ X. C. Lou,⁷³ S. Ye,⁷³ F. Bianchi,⁷⁴ M. Bona,⁷⁴ F. Gallo,⁷⁴ D. Gamba,⁷⁴ C. Borean,⁷⁵ L. Bosisio,⁷⁵ F. Cossutti,⁷⁵ G. Della Ricca,⁷⁵ S. Dittongo,⁷⁵ S. Grancagnolo,⁷⁵ L. Lanceri,⁷⁵ P. Poropat,^{75,‡} L. Vitale,⁷⁵ G. Vuagnin,⁷⁵ R. S. Panvini,⁷⁶ Sw. Banerjee,⁷⁷ C. M. Brown,⁷⁷ D. Fortin,⁷⁷ P. D. Jackson,⁷⁷ R. Kowalewski,⁷⁷ J. M. Roney,⁷⁷ H. R. Band,⁷⁸ S. Dasu,⁷⁸ M. Datta,⁷⁸ A. M. Eichenbaum,⁷⁸ J. J. Hollar,⁷⁸ J. R. Johnson,⁷⁸ P. E. Kutter,⁷⁸ H. Li,⁷⁸ R. Liu,⁷⁸ F. Di Lodovico,⁷⁸ A. Mihalyi,⁷⁸ A. K. Mohapatra,⁷⁸ Y. Pan,⁷⁸ R. Prepost,⁷⁸ S. J. Sekula,⁷⁸ P. Tan,⁷⁸ J. H. von Wimmersperg-Toeller,⁷⁸ J. Wu,⁷⁸ S. L. Wu,⁷⁸ Z. Yu,⁷⁸ and H. Neal⁷⁹

(BABAR Collaboration)

¹Laboratoire de Physique des Particules, F-74941 Annecy-le-Vieux, France

²Dipartimento di Fisica and INFN, Università di Bari, I-70126 Bari, Italy

³Institute of High Energy Physics, Beijing 100039, China

⁴University of Bergen, Institute of Physics, N-5007 Bergen, Norway

⁵Lawrence Berkeley National Laboratory and University of California, Berkeley, California 94720, USA

⁶University of Birmingham, Birmingham, B15 2TT, United Kingdom

⁷Ruhr Universität Bochum, Institut für Experimentalphysik I, D-44780 Bochum, Germany

⁸University of Bristol, Bristol BS8 1TL, United Kingdom

⁹University of British Columbia, Vancouver, BC, Canada V6T 1Z1

¹⁰Brunel University, Uxbridge, Middlesex UB8 3PH, United Kingdom

¹¹Budker Institute of Nuclear Physics, Novosibirsk 630090, Russia

¹²University of California at Irvine, Irvine, California 92697, USA

¹³University of California at Los Angeles, Los Angeles, California 90024, USA

¹⁴University of California at Riverside, Riverside, California 92521, USA

¹⁵University of California at San Diego, La Jolla, California 92093, USA

¹⁶University of California at Santa Barbara, Santa Barbara, California 93106, USA

¹⁷University of California at Santa Cruz, Institute for Particle Physics, Santa Cruz, California 95064, USA

¹⁸California Institute of Technology, Pasadena, California 91125, USA

¹⁹University of Cincinnati, Cincinnati, Ohio 45221, USA

²⁰University of Colorado, Boulder, Colorado 80309, USA

²¹Colorado State University, Fort Collins, Colorado 80523, USA

²²Technische Universität Dresden, Institut für Kern- und Teilchenphysik, D-01062 Dresden, Germany

²³Ecole Polytechnique, LLR, F-91128 Palaiseau, France

²⁴University of Edinburgh, Edinburgh EH9 3JZ, United Kingdom

²⁵Università di Ferrara, Dipartimento di Fisica and INFN, I-44100 Ferrara, Italy

- ²⁶Florida A&M University, Tallahassee, Florida 32307, USA
- ²⁷Laboratori Nazionali di Frascati dell'INFN, I-00044 Frascati, Italy
- ²⁸Dipartimento di Fisica and INFN, Università di Genova, I-16146 Genova, Italy
- ²⁹Harvard University, Cambridge, Massachusetts 02138, USA
- ³⁰Universität Heidelberg, Physikalisches Institut, Philosophenweg 12, D-69120 Heidelberg, Germany
- ³¹Imperial College London, London, SW7 2AZ, United Kingdom
- ³²University of Iowa, Iowa City, Iowa 52242, USA
- ³³Iowa State University, Ames, Iowa 50011-3160, USA
- ³⁴Laboratoire de l'Accélérateur Linéaire, F-91898 Orsay, France
- ³⁵Lawrence Livermore National Laboratory, Livermore, California 94550, USA
- ³⁶University of Liverpool, Liverpool L69 7ZE, United Kingdom
- ³⁷Queen Mary, University of London, E1 4NS, United Kingdom
- ³⁸University of London, Royal Holloway and Bedford New College, Egham, Surrey TW20 0EX, United Kingdom
- ³⁹University of Louisville, Louisville, Kentucky 40292, USA
- ⁴⁰University of Manchester, Manchester M13 9PL, United Kingdom
- ⁴¹University of Maryland, College Park, Maryland 20742, USA
- ⁴²University of Massachusetts, Amherst, Massachusetts 01003, USA
- ⁴³Laboratory for Nuclear Science, Massachusetts Institute of Technology, Cambridge, Massachusetts 02139, USA
- ⁴⁴McGill University, Montréal, Quebec, Canada H3A 2T8
- ⁴⁵Dipartimento di Fisica and INFN, Università di Milano, I-20133 Milano, Italy
- ⁴⁶University of Mississippi, University, Mississippi 38677, USA
- ⁴⁷Université de Montréal, Laboratoire René J. A. Lévesque, Montréal, Quebec, Canada H3C 3J7
- ⁴⁸Mount Holyoke College, South Hadley, Massachusetts 01075, USA
- ⁴⁹Dipartimento di Scienze Fisiche and INFN, Università di Napoli Federico II, I-80126, Napoli, Italy
- ⁵⁰NIKHEF, National Institute for Nuclear Physics and High Energy Physics, NL-1009 DB Amsterdam, The Netherlands
- ⁵¹University of Notre Dame, Notre Dame, Indiana 46556, USA
- ⁵²Oak Ridge National Laboratory, Oak Ridge, Tennessee 37831, USA
- ⁵³The Ohio State University, Columbus, Ohio 43210, USA
- ⁵⁴University of Oregon, Eugene, Oregon 97403, USA
- ⁵⁵Dipartimento di Fisica and INFN, Università di Padova, I-35131 Padova, Italy
- ⁵⁶Universités Paris VI et VII, Lab de Physique Nucléaire H.E., F-75252 Paris, France
- ⁵⁷Dipartimento di Elettronica and INFN, Università di Pavia, I-27100 Pavia, Italy
- ⁵⁸University of Pennsylvania, Philadelphia, Pennsylvania 19104, USA
- ⁵⁹Dipartimento di Fisica and INFN, Università di Perugia, I-06100 Perugia, Italy
- ⁶⁰Dipartimento di Fisica, Scuola Normale Superiore and INFN, Università di Pisa, I-56127 Pisa, Italy
- ⁶¹Prairie View A&M University, Prairie View, Texas 77446, USA
- ⁶²Princeton University, Princeton, New Jersey 08544, USA
- ⁶³Dipartimento di Fisica and INFN, Università di Roma La Sapienza, I-00185 Roma, Italy
- ⁶⁴Universität Rostock, D-18051 Rostock, Germany
- ⁶⁵Rutherford Appleton Laboratory, Chilton, Didcot, Oxon, OX11 0QX, United Kingdom
- ⁶⁶DSM/Dapnia, CEA/Saclay, F-91191 Gif-sur-Yvette, France
- ⁶⁷University of South Carolina, Columbia, South Carolina 29208, USA
- ⁶⁸Stanford Linear Accelerator Center, Stanford, California 94309, USA
- ⁶⁹Stanford University, Stanford, California 94305-4060, USA
- ⁷⁰State University of New York, Albany, New York 12222, USA
- ⁷¹University of Tennessee, Knoxville, Tennessee 37996, USA
- ⁷²University of Texas at Austin, Austin, Texas 78712, USA
- ⁷³University of Texas at Dallas, Richardson, Texas 75083, USA
- ⁷⁴Dipartimento di Fisica Sperimentale and INFN, Università di Torino, I-10125 Torino, Italy
- ⁷⁵Dipartimento di Fisica and INFN, Università di Trieste, I-34127 Trieste, Italy
- ⁷⁶Vanderbilt University, Nashville, Tennessee 37235, USA
- ⁷⁷University of Victoria, Victoria, British Columbia, Canada V8W 3P6
- ⁷⁸University of Wisconsin, Madison, Wisconsin 53706, USA
- ⁷⁹Yale University, New Haven, Connecticut 06511, USA
- (Received 8 December 2003; published 26 March 2004)

A search for the lepton-flavor-violating decay of the tau into three charged leptons has been performed using 91.5 fb^{-1} of data collected at an e^+e^- center-of-mass energy around 10.58 GeV with the BABAR detector at the SLAC storage ring PEP-II. In all six decay modes considered, the numbers of events found in data are compatible with the background expectations. Upper limits on the branching fractions are set in the range $(1-3) \times 10^{-7}$ at 90% confidence level.

Lepton-flavor violation (LFV) involving charged leptons has never been observed, and stringent experimental limits exist from muon branching fractions: $\mathcal{B}(\mu \rightarrow e\gamma) < 1.2 \times 10^{-11}$ [1] and $\mathcal{B}(\mu \rightarrow eee) < 1.0 \times 10^{-12}$ [2] at 90% confidence level (C.L.). Recent results from neutrino oscillation experiments [3] show that LFV does indeed occur, although the branching fractions expected in charged lepton decay due to neutrino mixing alone are probably no more than 10^{-14} [4].

In tau decays, the most stringent limit on LFV is $\mathcal{B}(\tau \rightarrow \mu\gamma) < 3.1 \times 10^{-7}$ at 90% C.L. [5]. Many extensions to the standard model (SM), particularly models seeking to describe neutrino mixing, predict enhanced LFV in tau decays over muon decays with branching fractions from 10^{-10} up to the current experimental limits [6]. Observation of LFV in tau decays would be a clear signature of non-SM physics, while improved limits will provide further constraints on theoretical models.

This analysis is based on data recorded by the *BABAR* detector at the PEP-II asymmetric-energy e^+e^- storage ring operated at the Stanford Linear Accelerator Center. The data sample consists of 81.9 fb^{-1} recorded at $\sqrt{s} = 10.58 \text{ GeV}$ and 9.6 fb^{-1} recorded at $\sqrt{s} = 10.54 \text{ GeV}$. With an expected cross section for tau pairs at the luminosity-weighted \sqrt{s} of $\sigma_{\tau\tau} = (0.89 \pm 0.02) \text{ nb}$ [7], this data sample contains over 160×10^6 tau decays.

The *BABAR* detector is described in detail in Ref. [8]. Charged-particle (track) momenta are measured with a five-layer double-sided silicon vertex tracker and a 40-layer drift chamber inside a 1.5-T superconducting solenoidal magnet. The transverse momentum resolution parametrized as $\sigma_{p_T}/p_T = (0.13 p_T / [\text{GeV}/c] + 0.45)\%$ is achieved. An electromagnetic calorimeter consisting of 6580 CsI(Tl) crystals is used to identify electrons and photons, a ring-imaging Cherenkov detector is used to identify charged hadrons, and the instrumented magnetic flux return (IFR) is used to identify muons. Particle attributes are reconstructed in the laboratory frame and then boosted to the e^+e^- center-of-mass (c.m.) frame using the measured asymmetric beam energies.

This Letter presents a search for LFV in the neutrinoless decay $\tau^- \rightarrow \ell^- \ell^+ \ell^-$. All possible lepton combinations consistent with charge conservation are considered, leading to six distinct decay modes ($e^-e^+e^-$, $\mu^+e^-e^-$, $\mu^-e^+e^-$, $e^+\mu^-\mu^-$, $e^-\mu^+\mu^-$, $\mu^-\mu^+\mu^-$) [9]. The signature of this process is three charged particles, each identified as either an electron or muon, with an invariant mass and energy equal to that of the parent tau lepton. Candidate signal events in this analysis are required to have a “1-3 topology,” where one tau decay yields three charged particles (3-prong), while the second tau decay yields one charged-particle (1-prong). Four well reconstructed tracks are required with zero net charge, pointing towards a common region consistent with $\tau^+\tau^-$ production and decay. One of these tracks must be separated from the other three by at least 90° in the c.m. frame. The plane perpendicular to this isolated track

divides the event into two hemispheres and defines the 1-3 topology. Pairs of oppositely charged tracks identified as photon conversions in the detector material with an e^+e^- invariant mass below $30 \text{ MeV}/c^2$ are ignored.

Each of the charged particles found in the 3-prong hemisphere must be identified as either an electron or a muon candidate. Electrons are identified using the ratio of calorimeter energy to track momentum (E/p), the ionization loss in the tracking system (dE/dx), and the shape of the shower in the calorimeter. Muons are identified by hits in the IFR and small energy deposits in the calorimeter. Muons with momentum less than $0.5 \text{ GeV}/c$ cannot be identified because they do not penetrate far enough into the IFR.

The particle identification (PID) requirements are not sufficient to suppress certain backgrounds, particularly those from higher-order radiative *Bhabha* and $\mu^+\mu^-$ events that can have four leptons in the final state. To reduce these backgrounds, additional selection criteria are applied to the six different decay modes. For all decay modes, the momentum of the 1-prong track is required to be less than $4.8 \text{ GeV}/c$ in the c.m. frame. For the $e^-e^+e^-$ and $e^-\mu^+\mu^-$ decay modes, the charged-particle in the 1-prong hemisphere must not be identified as an electron, while for the $\mu^-e^+e^-$ and $\mu^-\mu^+\mu^-$ decay modes it must not be a muon. For all four of these decay modes, the angle θ_{13} between the 1-prong momentum and the vector sum of the 3-prong momenta in the c.m. frame must satisfy $\cos\theta_{13} > -0.9999$, while the net transverse momentum of the four tracks must be greater than $0.1 \text{ GeV}/c$. Additional requirements are imposed to reduce the $q\bar{q}$ and SM $\tau^+\tau^-$ backgrounds. Events in the four decay modes specified above are required to have no unassociated calorimeter clusters (photons) in the 3-prong hemisphere with energy greater than 100 MeV in the laboratory frame, while events in all six decay modes are required to have no track in the 3-prong hemisphere that is also consistent with being a kaon.

To reduce backgrounds further, signal events are required to have an invariant mass and total energy in the 3-prong hemisphere consistent with a parent tau lepton. These quantities are calculated from the observed track momenta assuming the corresponding lepton masses for each decay mode. The energy difference is defined as $\Delta E \equiv E_{\text{rec}}^* - E_{\text{beam}}^*$, where E_{rec}^* is the total energy of the tracks observed in the 3-prong hemisphere and E_{beam}^* is the beam energy, both in the c.m. frame. The mass difference is defined as $\Delta M \equiv M_{\text{rec}} - m_\tau$ where M_{rec} is the reconstructed invariant mass of the three tracks and $m_\tau = 1.777 \text{ GeV}/c^2$ is the tau mass [10].

The signal distributions in the $(\Delta M, \Delta E)$ plane are broadened by detector resolution and radiative effects. The radiation of photons from the incoming e^+e^- particles before annihilation affects all decay modes, leading to a tail at low values of ΔE . Radiation from the final-state leptons is more likely for electrons than muons, and produces a tail at low values of ΔM as well. Rectangular

signal regions are defined separately for each decay mode as follows. For all six decay modes, the upper right corner of the signal region is fixed at $(30 \text{ MeV}/c^2, 50 \text{ MeV})$, while the lower left corner is at $(-70, -120)$ for the $e^-e^+e^-$ and $\mu^-e^+e^-$ decay modes, $(-100, -200)$ for $\mu^+e^-e^-$, $(-50, -200)$ for $e^+\mu^-\mu^-$, $(-50, -150)$ for $e^-\mu^+\mu^-$, and $(-30, -150)$ for $\mu^-\mu^+\mu^-$. All values are given in units of $(\text{MeV}/c^2, \text{MeV})$. These signal region boundaries are chosen to provide the smallest expected upper limits on the branching fractions in the background-only hypothesis. These expected upper limits are estimated using only MC simulations and data control samples, not candidate signal events. Figure 1 shows the observed data in the $(\Delta M, \Delta E)$ plane, along with the signal region boundaries and the expected signal distributions. To avoid bias, a blinded analysis procedure was adopted with the number of data events in the signal region remaining unknown until the selection criteria were finalized and all cross-checks were performed.

The efficiency of the selection for signal events is estimated with a MC simulation of LFV tau decays. Simulated tau-pair events including higher-order radiative corrections are generated using KK2F [7] with one tau decaying to three leptons with a three-body phase space distribution, while the other tau decays according to measured rates [11] simulated with TAUOLA [12]. Final-state radiative effects are simulated for all decays using PHOTOS [13]. The detector response is simulated with

GEANT4 [14], and the simulated events are then reconstructed in the same manner as data.

About 50% of the MC signal events pass the 1-3 topology requirement. The lepton identification efficiencies and misidentification probabilities are measured using tracks in kinematically selected data samples (radiative *Bhabha*, radiative $\mu^+\mu^-$, two-photon $e^+e^-\ell^+\ell^-$, and $J/\psi \rightarrow \ell^+\ell^-$) and parametrized as a function of particle momentum, polar angle, and azimuthal angle in the laboratory frame. These data-derived efficiencies are then used to give the probability that a simulated MC particle will be identified (or misidentified) as an electron or a muon. For the lepton momentum spectrum predicted by the signal MC events, the electron and muon identification requirements are found to have an average efficiency per lepton of 91% and 63%, respectively. The probability for a hadron to be misidentified as an electron in SM 3-prong tau decays is 2.2%, while the probability to be misidentified as a muon is 4.8% [15]. The final efficiency for signal events to be found in the signal region is shown in Table I for each decay mode and ranges from 7% to 12%. This efficiency includes the 85% branching fraction for 1-prong tau decays.

There are three main classes of background remaining after the selection criteria are applied: low multiplicity $q\bar{q}$ events (mainly continuum light-quark production), QED events (*Bhabha* and $\mu^+\mu^-$), and SM $\tau^+\tau^-$ events. These three background classes have distinctive distributions in the $(\Delta M, \Delta E)$ plane: $q\bar{q}$ events tend to populate the plane uniformly, while QED backgrounds are restricted to a narrow band at positive values of ΔE , and $\tau^+\tau^-$ backgrounds are restricted to negative values of

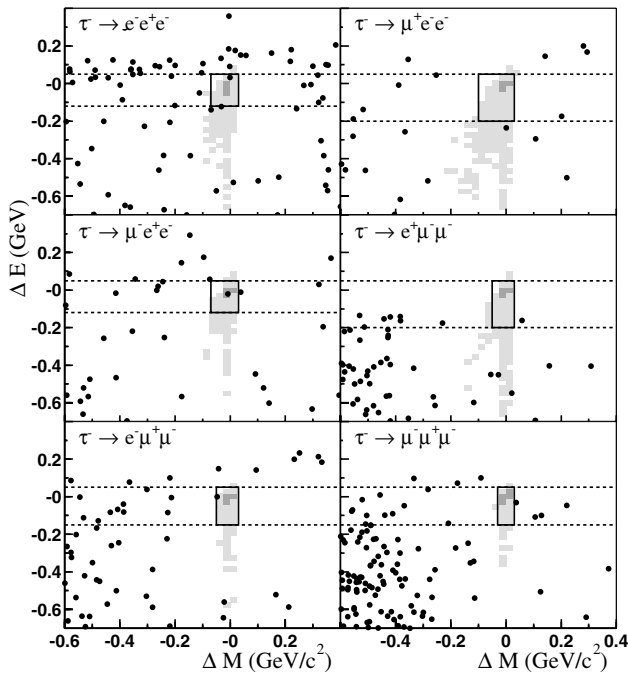


FIG. 1. Observed data shown as dots in the $(\Delta M, \Delta E)$ plane and the boundaries of the signal region for each decay mode. The dark and light shading indicates contours containing 50% and 90% of the selected MC signal events, respectively. The regions shown in Fig. 2 are indicated by dashed lines.

TABLE I. Efficiency estimates, number of expected background events (N_{bgd}), number of observed events (N_{obs}), and branching fraction upper limits for each decay mode.

Decay mode	$e^-e^+e^-$	$\mu^+e^-e^-$	$\mu^-e^+e^-$
Efficiency [%]	7.3 ± 0.2	11.6 ± 0.4	7.7 ± 0.3
$q\bar{q}$ bgd.	0.67	0.17	0.39
QED bgd.	0.84	0.20	0.23
$\tau^+\tau^-$ bgd.	0.00	0.01	0.00
N_{bgd}	1.51 ± 0.11	0.37 ± 0.08	0.62 ± 0.10
N_{obs}	1	0	1
$\mathcal{B}_{\text{UL}}^{90}$	2.0×10^{-7}	1.1×10^{-7}	2.7×10^{-7}
Decay mode	$e^+\mu^-\mu^-$	$e^-\mu^+\mu^-$	$\mu^-\mu^+\mu^-$
Efficiency [%]	9.8 ± 0.5	6.8 ± 0.4	6.7 ± 0.5
$q\bar{q}$ bgd.	0.20	0.19	0.29
QED bgd.	0.00	0.19	0.01
$\tau^+\tau^-$ bgd.	0.01	0.01	0.01
N_{bgd}	0.21 ± 0.07	0.39 ± 0.08	0.31 ± 0.09
N_{obs}	0	1	0
$\mathcal{B}_{\text{UL}}^{90}$	1.3×10^{-7}	3.3×10^{-7}	1.9×10^{-7}

both ΔE and ΔM . A negligible two-photon background remains.

The expected background rates for each decay mode are determined by fitting a set of probability density functions (PDFs) to the observed data in the $(\Delta M, \Delta E)$ plane in a grand sideband (GS) region. The GS region, shown in Fig. 1, is defined as the rectangle bounded by the points $(-600 \text{ MeV}/c^2, -700 \text{ MeV})$ and $(400 \text{ MeV}/c^2, 400 \text{ MeV})$, excluding the signal region. For both the $q\bar{q}$ and $\tau^+\tau^-$ backgrounds, an analytic PDF is constructed from the product of two PDFs P_M and P_E , where $P_M(\Delta M)$ is the sum of two Gaussians with a common mean and $P_E(\Delta E) = (1 - x/\sqrt{1+x^2})(1 + ax + bx^2 + cx^3)$ with $x = (\Delta E - d)/e$ [16]. The shapes of these PDFs are described by a total of nine free parameters, which are determined by fits to MC $q\bar{q}$ and $\tau^+\tau^-$ background samples for each decay mode.

For the QED backgrounds, an analytic PDF is constructed from the product of a Crystal Ball function [17] in $\Delta E'$ and a linear function in $\Delta M'$, where the $(\Delta M', \Delta E')$ axes have been rotated slightly from $(\Delta M, \Delta E)$ to fit the observed distribution. The six parameters of this PDF, including the rotation angle, are obtained by fitting control samples with a 1-3 topology that are enhanced in *Bhabha* or $\mu^+\mu^-$ events by requiring that the particle in the 1-prong hemisphere is identified as an electron or a muon. Any value for $\cos\theta_{13}$ is allowed, but the control sample events otherwise pass the selection criteria.

With the shapes of the three background PDFs determined, an unbinned maximum likelihood fit to the data in the GS region is used to find the expected rate of each background type in the signal region, as shown in Table I. The PDF shape determinations and background fits are performed separately for each of the six decay modes. Figure 2 shows the data and the background PDFs for values of ΔE in the signal range.

The largest systematic uncertainty in the signal efficiency is due to the uncertainty in measuring the PID

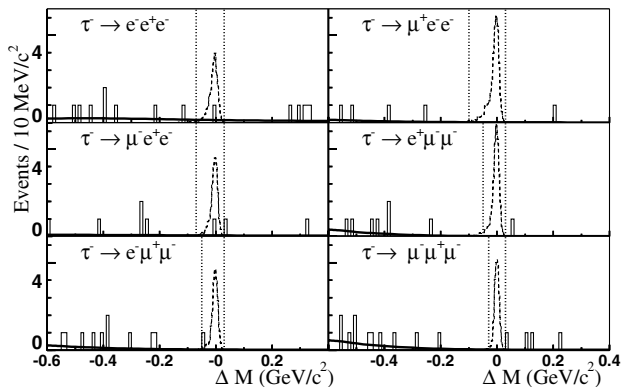


FIG. 2. Distribution of ΔM for data (solid histogram) and background PDFs (solid curves) for events with ΔE in the signal region indicated in Fig. 1. Expected signal distributions are shown (dashed histogram) for a branching fraction of 10^{-6} .

efficiencies. This uncertainty is determined from the statistical precision of the PID control samples, and ranges from 0.7% for $e^-e^+e^-$ to 6.2% for $\mu^-\mu^+\mu^-$ relative to the efficiency [18]. The modeling of the tracking efficiency contributes an additional 2% uncertainty, as does the statistical limitation of the MC signal sample. All other sources of uncertainty are found to be small, including the modeling in the generator of radiative effects, track momentum resolution, trigger performance, observables used in the selection criteria, and knowledge of the tau 1-prong branching fractions. The efficiency has been estimated using a three-body phase space model, and no uncertainty is assigned for possible model dependence. The selection efficiency is found to be uniform within 10% across the Dalitz plane, provided the invariant mass for any pair of leptons is less than $1.4 \text{ GeV}/c^2$.

Since the background levels are extracted directly from the data, systematic uncertainties on the background estimation are directly related to the background parametrization and the fit technique used. The finite data available in the GS region to determine the background rates are the largest uncertainties and vary from 10% to 25% depending upon the decay mode. Additional uncertainties are estimated by varying the fit procedure and changing the functional form of the background PDFs. Cross-checks of the background estimation were performed by considering the number of events expected and observed in sideband regions immediately neighboring the signal region for each decay mode.

The numbers of events observed (N_{obs}) and the background expectations (N_{bgd}) are shown in Table I, with no significant excess found in any decay mode. Upper limits on the branching fractions are calculated according to $\mathcal{B}_{\text{UL}}^{\text{90}} = N_{\text{UL}}^{\text{90}} / (2\varepsilon \mathcal{L} \sigma_{\tau\tau})$, where $N_{\text{UL}}^{\text{90}}$ is the 90% C.L. upper limit for the number of signal events when N_{obs} events are observed with N_{bgd} background events expected. The values ε , \mathcal{L} , and $\sigma_{\tau\tau}$ are the selection efficiency, luminosity, and $\tau^+\tau^-$ cross section, respectively. The estimates of $\mathcal{L} = 91.5 \text{ fb}^{-1}$ and $\sigma_{\tau\tau} = 0.89 \text{ nb}$ are correlated [19], and the uncertainty on the product $\mathcal{L}\sigma_{\tau\tau}$ is 2.3%. The branching fraction upper limits have been calculated including all uncertainties using the technique of Cousins and Highland [20] following the implementation of Barlow [21]. The 90% C.L. upper limits on the $\tau^- \rightarrow \ell^- \ell^+ \ell^-$ branching fractions, shown in Table I, are in the range $(1-3) \times 10^{-7}$. These limits represent an order of magnitude improvement over the previous experimental bounds.

We are grateful for the excellent luminosity and machine conditions provided by our PEP-II colleagues, and for the substantial dedicated effort from the computing organizations that support *BABAR*. The collaborating institutions thank SLAC for its support and kind hospitality. This work is supported by DOE and NSF (USA), NSERC (Canada), IHEP (China), CEA and CNRS-IN2P3 (France), BMBF and DFG (Germany), INFN (Italy), FOM (The Netherlands), NFR (Norway), MIST

(Russia), and PPARC (United Kingdom). Individuals have received support from the A. P. Sloan Foundation, Research Corporation, and Alexander von Humboldt Foundation.

*Also with Università della Basilicata, Potenza, Italy.

†Also with IFIC, Instituto de Física Corpuscular, CSIC-Universidad de Valencia, Valencia, Spain.

‡Deceased.

- [1] MEGA/LAMPF Collaboration, M. L. Brooks *et al.*, Phys. Rev. Lett. **83**, 1521 (1999).
- [2] SINDRUM Collaboration, U. Bellgardt *et al.*, Nucl. Phys. **B299**, 1 (1998).
- [3] K2K Collaboration, M. H. Ahn *et al.*, Phys. Rev. Lett. **90**, 041801 (2003); KamLAND Collaboration, K. Eguchi *et al.*, Phys. Rev. Lett. **90**, 021802 (2003); SNO Collaboration, Q. R. Ahmad *et al.*, Phys. Rev. Lett. **89**, 011301 (2002); Super-Kamiokande Collaboration, Y. Fukuda *et al.*, Phys. Rev. Lett. **81**, 1562 (1998).
- [4] X. Y. Pham, Eur. Phys. J. C **8**, 513 (1999).
- [5] Belle Collaboration, K. Abe *et al.*, hep-ex/0310029.
- [6] E. Ma, Nucl. Phys. B, Proc. Suppl. **123**, 125 (2003).
- [7] B. F. Ward, S. Jadach, and Z. Was, Nucl. Phys. B, Proc. Suppl. **116**, 73 (2003).
- [8] BABAR Collaboration, B. Aubert *et al.*, Nucl. Instrum. Methods Phys. Res., Sect. A **479**, 1 (2002).
- [9] Throughout this Letter, charge conjugate decay modes also are implied.
- [10] BES Collaboration, J. Z. Bai *et al.*, Phys. Rev. D **53**, 20 (1996).
- [11] Particle Data Group, K. Hagiwara *et al.*, Phys. Rev. D **66**, 010001 (2002).
- [12] S. Jadach, Z. Was, R. Decker, and J. H. Kuhn, Comput. Phys. Commun. **76**, 361 (1993).
- [13] E. Barberio and Z. Was, Comput. Phys. Commun. **79**, 291 (1994).
- [14] GEANT4 Collaboration, S. Agostinelli *et al.*, Nucl. Instrum. Methods Phys. Res., Sect. A **506**, 250 (2003).
- [15] Because of the need to identify three leptons, the PID requirements emphasize efficiency over purity, resulting in a relatively high misidentification rate.
- [16] OPAL Collaboration, G. Abbiendi *et al.*, Phys. Lett. B **492**, 23 (2000).
- [17] Crystal Ball Collaboration, T. Skwarnicki, Report No. DESY-F31-86-02, 1986.
- [18] All uncertainties quoted in the text are relative.
- [19] The luminosity is measured using the observed $\mu^+\mu^-$ rate, and the $\mu^+\mu^-$ and $\tau^+\tau^-$ cross Secs. are both estimated with KK2F.
- [20] R. D. Cousins and V. L. Highland, Nucl. Instrum. Methods Phys. Res., Sect. A **320**, 331 (1992).
- [21] R. Barlow, Comput. Phys. Commun. **149**, 97 (2002).